DOI: 10.1002/ejic.200801224

Synthesis and Structure Characterization of Copper Terephthalate Metal–Organic Frameworks

Cantwell G. Carson,[a] Kenneth Hardcastle,[b] Justin Schwartz,[c,d] Xiaotao Liu,[d] Christina Hoffmann,[e] Rosario A. Gerhardt,[a] and Rina Tannenbaum*[a,f]

Keywords: Microporous materials / Coordination polymers / Crystal engineering / Magnetic properties / Carboxylate ligands / Metal-organic frameworks

In this paper, we report on a high-throughput (gram quantities) solvothermal method for the synthesis of copper terephthalate metal–organic frameworks in dmf. While the structure of MOF-2 and some of the associated polymorphs are well known, we know of no equivalent structural studies for the isostructural copper terephthalate (Cu–tpa). The material we have made crystallizes in the *C*2/*m* space group. Cu–tpa also exhibits reversible solvent-exchange properties. These properties make this material useful for potential applications in gas storage and catalysis applications.

Introduction

The term metal–organic framework (MOF) describes a class of materials in which organic, polyfunctional ligands form coordination bonds with multiple metal atoms to form extended polymeric structures in one-, two-, and three dimensions. They are often crystalline, highly porous, and resistant to structural collapse upon evacuation.[1] The variation of the ligand character, functionality, spacer length, metal atom, and synthesis environment has given rise to the formation of a large number of porous compounds with a correspondingly large variety of properties and applications.[2] Here, we report a high-throughput synthesis that generates gram quantities of a copper terephthalate MOF along with the associated crystal structure, surface area, and *anti*-ferromagnetic susceptibility.

The synthesis of metal terephthalate complexes from metal salt and terephthalic acid (tpaH) dates as far back as 1967, with a nickel terephthalate compound synthesized by Acheson and Galwey.[3] Other hydrated metal terephthalates (Fe, Cr, Co, Cu, Ag, Mn, La) were synthesized by Sherif.[4] It was not until recently, however, that advances in single-crystal diffraction and computational refinement allowed adequate structural determination of these insoluble crystalline solids. Subsequent structural determination has allowed investigation of metal terephthalates as porous metal–organic frameworks. One of the early metal terephthalate complexes characterized as porous MOFs was a copper terephthalate trihydrate Cu(tpa)·3(H_2O) synthesized by Cueto et al.,[5] which was further studied for conductivity and magnetic susceptibility.[6] The first copper terephthalate with a large surface area was reported by Mori et al.[7,8] The presumed structure was one of a paddlewheel, but no structure was ever provided. There have been mono- and dihydrated copper terephthalate complexes reported by Deakin et al.,[9a,9b] but these structures have different coordination geometries and they lack the lamellar, paddlewheel coordination geometry predicted by Mori. One attempt at the solvothermal synthesis of the paddlewheel copper terephthalate complex yielded Cu(tpa)·($NHMe_2$)$_2$, achieved by the hydrolysis of dmf during synthesis.[10] This latter complex has a structure similar to that of Cu(tpa)(OH)$_2$, previously synthesized by Deakin. Another similar structure is that of Cu(1,3-BDC)·(H_2O) reported by Gao.[11]

Research groups have since used copper terephthalate as a platform for the construction of MOFs with larger porosities, by incorporating triethylenediamine[12] and dimethylamine;[10] however, we know of no published structure of copper terephthalate. As applications of MOFs for catalysis are investigated, MOFs with open coordination sites, like

[a] School of Materials Science and Engineering, Georgia Institute of Technology,
Atlanta, GA 30332, USA
Fax: +1-404-894-1940
E-mail: rina.tannenbaum@mse.gatech.edu
[b] Department of Chemistry, Emory University,
Atlanta, GA 30322, USA
[c] National High Magnetic Field Laboratory, Florida State University,
Tallahassee, FL 32310, USA
[d] Department of Mechanical Engineering, Florida A&M University-Florida State University College of Engineering,
Tallahassee, FL 32310, USA
[e] Spallation Neutron Source, NSSD / ORNL,
Oak Ridge, TN 37831, USA
[f] Department of Chemical Engineering, Technion – Israel Institute of Technology, Technion City,
Haifa 32000, Israel
Supporting information for this article is available on the WWW under http://www.eurjic.org or from the author.

copper terephthalate, will likely be scrutinized for possessing both homogeneous and heterogeneous catalytic behavior.[13] The Cu(tpa) MOF, though similar to MOF-2, exhibits a markedly higher surface area, which makes it a superior candidate for gas separation and sieving applications. Unlike MOF-2, the magnetic properties of Cu(tpa) also render it an attractive template for the development of high-surface-area magnetic materials.

Unfortunately, the lack of a high-throughput synthesis, i.e. a process whereby gram or kilogram quantities can be synthesized in a matter of hours at ambient pressure, has thus far been an impediment in the study of novel applications for copper terephthalate frameworks. Formerly, many MOFs were synthesized in water or through slow-diffusion methods. While these are effective, these approaches have drawbacks. The dehydration of hydrated metal terephthalates often leads to the collapse of the crystal structure and the associated surface area. Many of the non-aqueous synthesis methods involve slow-diffusion processes that take days or weeks to complete, which eliminates the possibility of an industrially relevant process. Other alternatives involve the use of an autoclave, which is not desirable from an industrial standpoint.

Recently, *N*,*N*-dimethylformamide (dmf) has become popular as a solvent for MOF synthesis because of its high boiling point and ability to dissolve carboxylic acids and metal salts. Yaghi's group used a room-temperature synthesis in dmf to create MOF-2 in 1998.[14] This zinc terephthalate complex was structurally similar to the copper terephthalate developed by Mori et al. and was the first in a long line of high-surface-area zinc dicarboxylate materials. A solvothermal version was later developed by BASF.[15] Other groups have used electrochemical methods to speed up the synthesis.[16]

Although the structure of MOF-2 and some of the associated polymorphs are well studied,[17,18] we know of no equivalent high-throughput syntheses for the isostructural copper terephthalate. Along similar lines to that used for MOF-2, we have used dmf at elevated temperatures to carry out the reaction shown in Equation (1).

$$Cu(NO_3)_2 + C_6H_4(COOH)_2 \xrightarrow[\text{air,110°C}]{\text{dmf}} Cu[C_6H_4(COO)_2](dmf) + 2HNO_3 \quad (1)$$

If high-quality crystal growth is desired, a sealed container will facilitate the deprotonation of the terephthalic acid by forcing the hydrolyzed dimethylamine base into solution with the solvent. However, synthesis in a stirred round-bottomed flask yields a powder with identical properties and structure. With the structure known, large quantities can be confidently synthesized without great difficulty. We anticipate that this high-throughput synthesis and the details of the associated crystal structure prior to activation will pave the way for applications development and comparison among similarly synthesized MOFs.

Results and Discussion

Analysis of the single crystals of the resulting blue powder generated by this synthesis yielded a framework of Cu(tpa)·(dmf), depicted in Figure 1. In this complex, terephthalate ligands are coordinated in a bidentate bridging fashion to a Cu^{II} dimer, separated vertically by 2.63 Å. Each Cu^{II} atom is also coordinated to a molecule of dmf to give the Cu^{II} atoms a square-pyramidal coordination geometry. This leads to a structure in which the Cu^{II} atoms are coordinated to the tpa linkers in the ($\bar{2}$01) planes. These sheets are then bonded through weak stacking interactions, similar to those in MOF-2.[14] Clausen et al. reported the structure of a polymorph of MOF-2 that has the same space group and similar unit-cell parameters.[17]

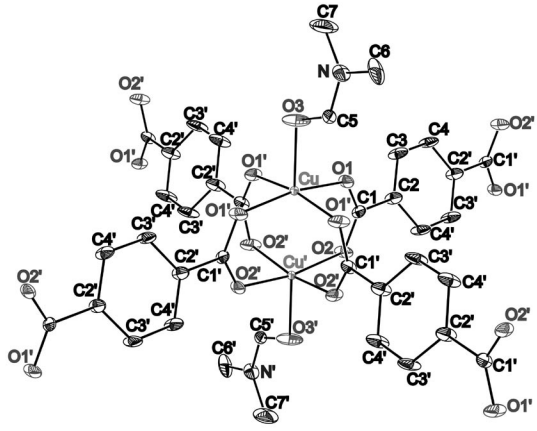

Figure 1. The crystal structure for Cu(tpa)·(dmf) illustrates the sheetlike properties of the structure.

We carried out X-ray powder diffraction experiments to verify the crystal structure assignment of Cu(tpa)·(dmf) and to examine the effect of temperature and solvent on the crystal structure. These diffraction patterns (Figure 2) show a clear match between the predicted powder diffraction pattern and the experimental pattern. For the powder diffraction trace of the "dried" powder, Cu(tpa)·(dmf) was placed in a high-temperature X-ray diffraction oven and dried at 220 °C. The powder diffraction was measured in situ (vide infra) under a He atmosphere. Desolvated Cu(tpa) powder was then washed in *N*-methylpyrrolidone (nmp) at 120 °C for 30 min. After this treatment, the washed powder has a powder diffraction pattern that is almost identical to that of original Cu(tpa)·(dmf). This indicates that, like dmf, nmp coordinates to Cu^{II} through the carbonyl group. We also exposed the desolvated Cu(tpa) to a similar treatment in ethanol, by heating at reflux for 30 min. The effect of the treatment in ethanol was different than when dmf or nmp was used, as the diffraction pattern appears to become a more amorphous version of the original desolvated structure. This indicates that the ethanol, which lacks the carbonyl group, does not coordinate to the Cu atom in the same way that dmf and nmp coordinate. Selectivity for coordinating certain functional groups over others would make Cu(tpa) a candidate for molecular sieving and gas separation applications. This also indicates that

the structure could be modified by exposure to different solvents by tailoring the chemical properties and bond strength between adjacent Cu(tpa) sheets. Consistent with the thermogravimetric and IR analyses, the crystal structure undergoes a phase change between 160 and 220 °C (Figure 3). Moreover, this phase remains unchanged above 300 °C.

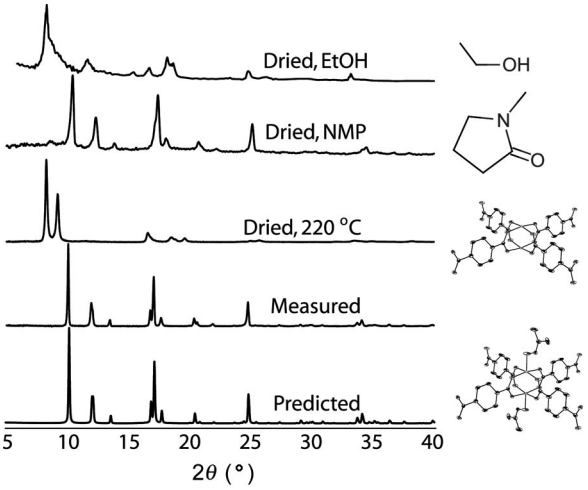

Figure 2. The X-ray diffraction patterns of Cu(tpa)·(dmf) under various conditions. The scan labeled "predicted" is the predicted powder pattern based on the single-crystal structural assignment. The measured powder diffraction pattern at room temperature before desolvation is labeled as "measured" and after as "dried, 220 °C". For "dried, nmp", Cu(tpa) has been re-wetted with *N*-methylpyrrolidone and has a diffraction pattern that is similar to that of the original Cu(tpa)·(dmf). As shown in the pattern "dried, EtOH", when dry Cu(tpa) is immersed in ethanol, it appears to lose crystallinity instead of returning to the original Cu(tpa)·(dmf) crystal structure.

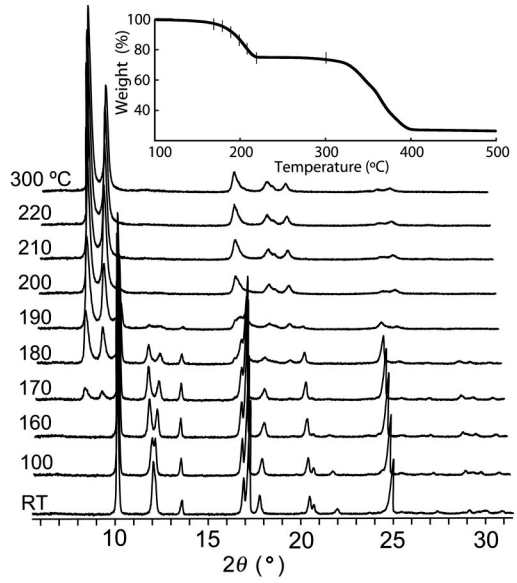

Figure 3. A series of powder diffraction scans is shown, which details the change in the crystal structure as a function of thermal desolvation. The first three scans from the bottom were taken at room temperature, 100, and 160 °C. These show little change in the crystal structure, aside from a separation of the (001) and (020) peaks. The next seven scans are taken at intervals of 10 °C from 160 to 220 °C. Between these temperatures the solvated Cu(tpa)·(dmf) crystal structure changes to that of desolvated Cu(tpa). The last scan, taken at 300 °C, shows that the structure Cu(tpa) remains unchanged up to 300 °C. The inset shows the thermogravimetric profile with marks that indicate the temperatures at which a powder diffraction profile was recorded.

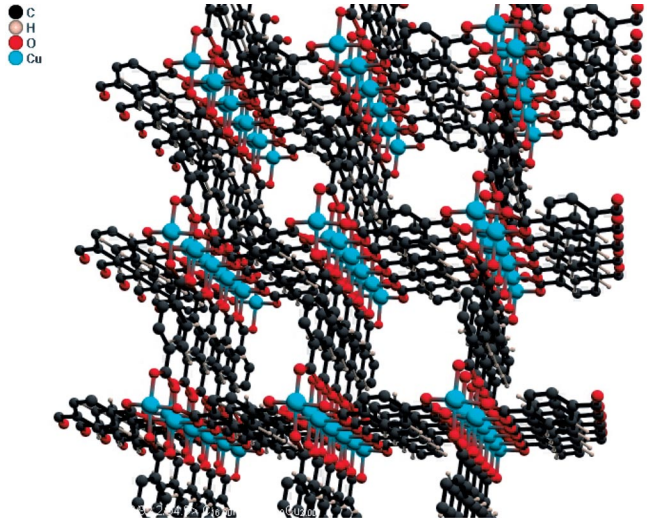

Figure 4. A hypothetical view of the desolvated Cu(tpa) structure, which illustrates the stacking of lamellar structures that are covalently bonded in the (001) plane to form associated channels that provide the high surface area.

Figure 4 depicts the channels that are believed to form upon thermal desolvation of Cu(tpa)·(dmf) to Cu(tpa). Unfortunately, there were no crystals of sufficient quality to perform single-crystal analysis, as the process of desolvation leaves only a fine powder. Moreover, the peaks in the powder pattern appear to be broadened by the small crystallite size. As a result, the structure of the desolvated Cu(tpa) could not be solved through conventional methods. However, on the basis of the similarity it shares with copper *trans*-1,4-cyclohexanedicarboxylate, we suspect that it has a similar structure.[19] Work is currently being done to solve the structure of desolvated Cu(tpa) through simulation.

The dmf molecule present after synthesis can be removed through thermal desorption, to yield a desolvated structure, which is referred to as Cu(tpa). The thermogravimetric profile shows a clear weight-loss step starting at 160 and ending at 220 °C. This weight loss of 26% corresponds well to the loss of one solvent molecule per monomer. The stability of the phase above 220 °C is indicated by the fact that there is no significant weight change until pyrolysis at 325 °C. IR measurements were carried out to confirm the loss of solvent at 180 °C. The results of these measurements, along with their corresponding assignments, are shown in Table 1. After the sample was dried at 100 °C, its IR spectrum shows peaks corresponding to both Cu(tpa) and dmf. After the sample was dried at 225 °C to thoroughly remove any residual dmf present in the structure, the IR peaks corresponding to dmf can no longer be seen, while that for Cu(tpa) is still very visible. The dmf ν(CO) band appears to be red-shifted from the usual value of 1676 cm^{-1} for the free mole-

cule to 1662 cm^{-1} for a molecule that is coordinated to the Cu^{II} center. The band for the asymmetric stretch of the carboxylate group of tpa, ν_a(COO), also appears to be blue-shifted in the presence of dmf. After removal of dmf at 225 °C, the ν_a(COO) band redshifts from 1603 cm^{-1} to 1576 cm^{-1}. It appears that, if the solid is left in air, the Cu(tpa)·(dmf) solid will lose some of the coordinated solvent over a period of months, causing some of the peak locations to drift.

Table 1. Selected IR frequencies and their assignment to Cu(tpa) or dmf.[a]

Before drying			After drying	
Wavenumber (cm^{-1})	Assignment dmf[24]	Assignment Cu(tpa)[25]	Wavenumber (cm^{-1})	Assignment Cu(tpa)[25]
1663	ν(CO)		–	
1603		ν_a(COO)	1576	ν_a(COO)
1507		19a	1506	19a
1438	$\delta_s(CH_3)$		–	
1385	δ(CH)	ν_s(COO)	1387	ν_s(COO)
1316		14	1320	14
1257	ν_a(C′N)		–	
1104	$r(CH_3)$ ip		–	
1063	δ(CH) op		–	
1015		18a	1018	18a
882	ν_s(C′N)	11	877	11
730		12	734	12
675	δ(OCN)		–	

[a] Definitions: ν: stretching; δ: planar angle bending; r: rocking; a: asymmetric; s: symmetric; ip: in plane; op: out of plane. The numbers 19a, 14, 18a, 11 and 12 represent the Wilson notation used to describe phenyl vibrations.

Gas sorption experiments were performed to estimate the effect of the removal of dmf on the microporosity and on the accessible internal surface area of the metal–organic framework. Sorption with N_2 at 77 K revealed that the evacuated structure shows a type I isotherm (shown in Figure 5) with a BET surface area of 625 $m^2 g^{-1}$, a Langmuir surface area of 752 $m^2 g^{-1}$, and a micropore volume of 0.282 $cm^3 g^{-1}$. The monolayer volume of 181 $cm^3 g^{-1}$ (at STP) indicates that the uptake of N_2 at 77 K is 22.8% on a mass basis. These values compare favorably with the surface areas of 545 and 708 $m^2 g^{-1}$ for the BET and Langmuir surface areas, respectively, reported by Seki for Cu(tpa) synthesized in methanol.[8] It is interesting to note that while Cu(tpa) and MOF-2 are structurally similar in many aspects, Cu(tpa) exhibits a Langmuir surface area and micropore volume that is roughly double that of MOF-2 (270 $m^2 g^{-1}$ and 0.093 $cm^3 g^{-1}$, respectively, for MOF-2).[14] Cu(tpa) is also similar to the copper trimesate HKUST-1 reported by Chui.[20] The principal difference is that HKUST-1 is coordinated in three dimensions to create empty FCC cubes with large square pores, whereas Cu(tpa) appears to have a lamellar geometry that forms two-dimensional tunnels. Although Cu(tpa) has about half the surface area of HKUST-1,[21] it may be desired if confinement to one dimension is required or if a comparison to determine the effect of pore geometry on a particular materials property is to be made.

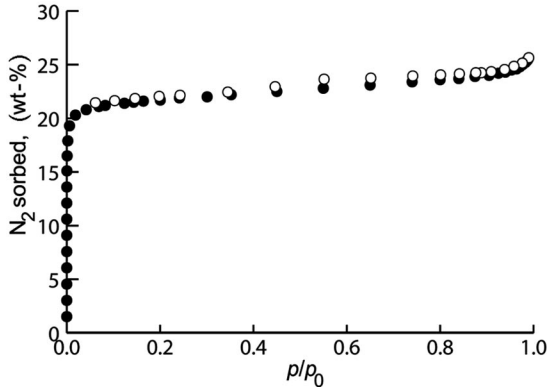

Figure 5. The BET isotherm of Cu(tpa) at 77 K after evacuation is of type I. The filled circles denote the uptake upon adsorption and the empty circles the release upon desorption. The curve shows very little hysteresis, which indicates reversible gas storage. The associated BET surface area is 625 $m^2 g^{-1}$ and the Langmuir surface area is 752 $m^2 g^{-1}$.

Magnetization experiments were carried out to examine the magnetic susceptibility of Cu(tpa)·(dmf). The results, shown in Figure 6, indicate a strong antiferromagnetic coupling between adjacent metal centers with a small paramagnetic impurity. The temperature dependence of the molar susceptibility was modeled with the Bleaney–Bowers equation as modified by Kahn, shown in Equation (2).[22]

$$\chi_M = \frac{2N_a g^2 \mu_B{}^2}{kT}\left\{\left[3+\exp\left(\frac{-J}{kT}\right)\right]^{-1}(1-\rho)+\frac{\rho}{4}\right\} \quad (2)$$

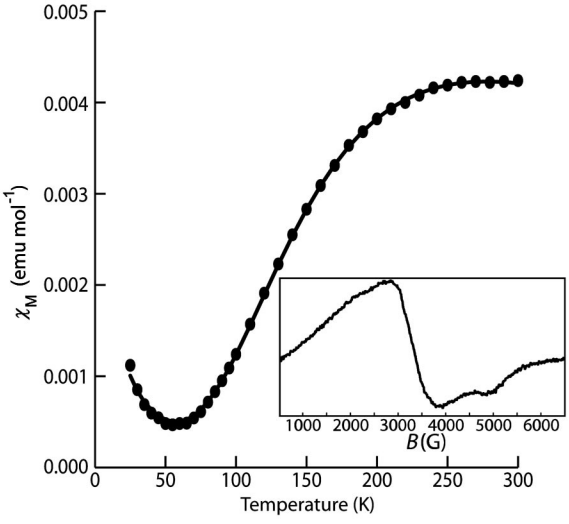

Figure 6. The magnetic susceptibility of Cu(tpa)·(dmf) shows paramagnetic behavior below 50 K and antiferromagnetic behavior above. The fitted curve indicates that Cu(tpa)·(dmf) has the values g = 2.2 and $-J$ = 331 cm^{-1}. The inset shows the room-temperature field swept X-band EPR spectrum of solid, dry Cu(tpa) after desolvation. The primary resonance is centered around g = 2.12. Experimental conditions: frequency 9.87 GHz; time constant 1.31 s; conversion time 169 ms; modulation amplitude 0.50 G; modulation frequency 100 kHz; microwave power 0.633 mW; data acquisition time 11 min.

In Equation (2), the spin Hamiltonian used is $\hat{H} = -JS_1S_2$. $\hat{H}$ denotes the operation between the singlet and triplet spin states (S_1 and S_2, respectively) in the Cu dimer, and $-J$ is a measure of the energy difference that arises between those two degenerate states in the presence of a magnetic field. N_a, g, μ_B, k, and T have the usual meanings as the Avogadro constant, gyromagnetic factor of the free electron, Bohr magneton, Boltzmann coefficient, and sample temperature, respectively. The symbol ρ denotes the fraction of uncoupled paramagnetic impurity atoms present in the sample. The line of best fit indicates $J = -311$ cm^{-1} and $\rho = 1.1\%$. As shown in the inset of Figure 6, X-band EPR spectroscopy was used to measure the g-factor directly. This can be done with $g = (h\nu/\mu_B H)$ where h, ν, and H are Planck's constant, the measurement frequency, and the magnetic field, respectively. This calculation yields a value of $g = 2.12$ for the largest radical with a small radical centered at $g = 1.53$, which is attributed to an impurity. The values for $-J$ and g are consistent with other Cu dimer complexes, including the similar compound synthesized by Mori.[23,7]

Conclusions

The results presented in this article indicate that the high-throughput synthesis of copper nitrate and terephthalic acid in dmf can be used to generate large amounts of the copper terephthalate metal–organic framework with antiferromagnetic coupling. Desolvation at high temperature of this material results in a product with a surface area comparable to those of other high-surface-area materials. These properties make it a compelling candidate for application in gas separation and sieving. The presence of the copper atom and its exposed apical coordination site might also lead to catalysis applications. The similarities of Cu(tpa)·(dmf) to other related frameworks indicate that novel magnetic materials could be synthesized by the introduction of a heterometallic center to the dimer. If the interest in MOFs such as HKUST-1 and MOF-2 is any indication, then the synthesis method described here may have a very broad impact on the development of MOFs with a potentially wide array of applications. We have been working on a computational solution to the desolvated powder pattern and expect to publish it shortly in a separate article.

Experimental Section

To synthesize Cu(tpa)·(dmf), equimolar quantities of copper nitrate trihydrate (Aldrich, 1.053 g) and terephthalic acid (Aldrich, 0.724 g) were dissolved in dmf (Aldrich, 87 mL). This solution was placed in a closed scintillation flask in an oven at 110 °C for 36 h. Small blue precipitated crystals were visible inside the flask upon removal from the oven. After repeated centrifugation and washing, the yield was 80%. Microanalysis (Atlantic Microlab, Norcross, GA) demonstrated a close agreement between the synthesized compound and the empirical formula. $C_{11}H_{11}CuNO_5$ (300.76): calcd. C 43.93, H 3.69, N 4.66, O 26.60; found C 43.33, H 3.67, N 4.67, O 26.49. Upon drying at 225 °C, the analyses were for $C_8H_4CuO_4$ (227.66): calcd. C 42.21, H 1.77, N 0.00, O 28.11; found C 40.83, H 1.81, N 0.16, O 27.81. The remaining portions should have been Cu, but the microanalyses indicated a small amount of impurities in the original specimen (calcd. Cu 21.13; found 21.85) and a much larger impurity content in the specimen desolvated at 225 °C (calcd. 27.91; found 29.41). Synthesis of Cu(tpa)·(dmf) in a round-bottomed flask with a stirrer at 125 °C in air for 24 h led to a powder with a smaller crystallite size, but identical properties otherwise.

The crystal structure of blue block-shaped crystals of Cu(tpa)·(dmf) were analyzed at 173 K: monoclinic, space group $C2/m$ with $a = 11.4143(3)$ Å, $b = 14.2687(4)$ Å, $c = 7.7800(2)$ Å, $\beta = 108.119(1)°$, $V = 1204.27(6)$ Å^3, $Z = 4$, $d_{calcd.} = 1.637$ g cm^{-3} and μ_a (Mo-K_α) = 1.824 mm^{-1}. Data collection was carried out at 173 K on a Bruker D8 SMART APEX CCD sealed tube diffractometer by using Mo-K_α radiation with a graphite monochromator and ω scans out to 25.96°, which gives 1159 unique reflections. The structure was solved by direct methods (SHELXTL, V6.12) and refined to a standard discrepancy index of $R = 0.0348$ and $R_w = 0.0818$ for 1046 reflections with $F > 2\sigma(F)$ and a goodness of fit on $F^2 = 1.093$. Anisotropic thermal parameters were refined for all non-hydrogen atoms; hydrogen atoms were refined isotropically as riding atoms. Some of the hydrogen atoms could not be resolved, and thus were not included in the analysis. CCDC-687690 contains the supplementary crystallographic data for this paper. These data can be obtained free of charge from The Cambridge Crystallographic Data Centre via www.ccdc.cam.ac.uk/data_request/cif.

Powder diffraction scans were taken with a Rigaku Mini-Flex with Cu-K_α with factory default settings. High-temperature powder diffraction scans were taken with a Panalytical X′Pert Pro MPD with Cu-K_α radiation. The Anton-Parr HTK 1200 oven furnace was used to control the temperature under a He atmosphere. Exposure of the desolvated product led to the formation of diffraction peaks not otherwise seen. X′Pert Highscore Plus was used to refine the single-crystal parameters to the measured powder diffraction profile. Thermogravimetric analyses were carried out with a TA Instruments Q50 Thermogravimetric Analyzer on a sample of 36 mg at a rate of 1 °C min^{-1}. Surface area measurements were obtained with a Micromeritics ASAP 2020. For the magnetic susceptibility measurements, a Quantum Design SQUID magnetometer was used with a background magnetic field of 100 Oe and a sample size of 1 gram. Room-temperature X-band electron paramagnetic resonance measurements were carried out with a X-band Bruker EMX Spectrometer (9.872 GHz) equipped with a Bruker HS4119 high-sensitivity cavity with power 0.633 mW, modulation frequency 100 kHz, time constant 1.31 s, conversion time 169 ms, modulation amplitude 0.50 G, and a data acquisition time 11 min.

Supporting Information (see footnote on the first page of this article): The infrared spectrum of Cu(tpa) is shown both before desolvation, Cu(tpa)·(dmf), and after, Cu(tpa).

Acknowledgments

We thank Jason Ward and the laboratory of Dr. William Koros for their assistance with the surface area measurements. Thanks also to the staff at the Center for Nanophase Materials Science at Oak Ridge National Laboratory for use of their Panalytical X'Pert PRO-MPD High Temperature X-ray diffraction equipment. We also thank David Jenson and the laboratory of Dr. Bridgette Barry for their assistance with the EPR measurements. This work was supported by a generous graduate fellowship from the Institute for Paper Science and Technology at the Georgia Institute of Technology (to C. G. C.), the Department of Energy grant DE-FG-02-03-

ER 46035 (to R. G.), and by the European Union Marie Curie International Reintegration Grant (IRG), Nr. 036577 (to R. T.).

[1] a) G. Ferey, C. Mellot-Draznieks, C. Serre, F. Millange, *Acc. Chem. Res.* **2005**, *38*, 217–225; b) H. Li, M. Eddaoudi, M. O'Keeffe, O. M. Yaghi, *Nature* **1999**, *402*, 276–279.
[2] a) D. Maspoch, D. Ruiz-Molina, K. Wurst, N. Domingo, M. Cavallini, F. Biscarini, J. Tejada, C. Rovira, J. Veciana, *Nat. Mater.* **2003**, *2*, 190–195; b) W. Mori, S. Takamizawa, C. N. Kato, T. Ohmura, T. Sato, *Microporous Mesoporous Mater.* **2004**, *73*, 31–46; c) R. Tannenbaum, *J. Mol. Catal. A* **1996**, *107*, 207–215; d) Z. T. Xu, *Coord. Chem. Rev.* **2006**, *250*, 2745–2757.
[3] R. J. Acheson, A. K. Galwey, *J. Chem. Soc. A* **1967**, 1174–1178.
[4] F. G. Sherif, *Ind. Eng. Chem. Res.* **1970**, *9*, 408–412.
[5] S. Cueto, V. Gramlich, W. Petter, F. S. Rys, P. Rys, *Acta Crystallogr., Sect. C: Cryst. Struct. Commun.* **1991**, *47*, 75–78.
[6] S. Cueto, P. Rys, F. S. Rys, R. Sanjinez, H. P. Straumann, *J. Magn. Magn. Mater.* **1992**, *104*, 1096–1097.
[7] W. Mori, F. Inoue, K. Yoshida, H. Nakayama, S. Takamizawa, M. Kishita, *Chem. Lett.* **1997**, 1219–1220.
[8] K. Seki, S. Takamizawa, W. Mori, *Chem. Lett.* **2001**, *30*, 122–123.
[9] a) L. Deakin, A. M. Arif, J. S. Miller, *Inorg. Chem.* **1999**, *38*, 5072–5077; b) J. A. Kaduk, *Acta Crystallogr., Sect. B: Struct. Sci.* **2002**, *58*, 815–822.
[10] S. M. Hawxwell, L. Brammer, *Crystengcomm* **2006**, *8*, 473–476.
[11] L. Gao, B. J. Zhao, G. H. Li, Z. Shi, S. H. Feng, *Inorg. Chem. Commun.* **2003**, *6*, 1249–1251.
[12] K. Seki, *Chem. Commun.* **2001**, *30*, 1496–1497.
[13] L. Alaerts, E. Seguin, H. Poelman, F. Thibault-Starzyk, P. A. Jacobs, D. E. De Vos, *Chem. Eur. J.* **2006**, *12*, 7353–7363.
[14] H. Li, M. Eddaoudi, T. L. Groy, O. M. Yaghi, *J. Am. Chem. Soc.* **1998**, *120*, 8571–8572.
[15] U. Mueller, M. Schubert, F. Teich, H. Puetter, K. Schierle-Arndt, J. Pastre, *J. Mater. Chem.* **2006**, *16*, 626–636.
[16] a) A. Domenech, H. Garcia, M. T. Domenech-Carbo, F. Llabres-i-Xamena, *Electrochem. Commun.* **2006**, *8*, 1830–1834; b) A. Domenech, H. Garcia, M. T. Domenech-Carbo, F. Llabres-I-Xamena, *J. Phys. Chem. C* **2007**, *111*, 13701–13711.
[17] H. F. Clausen, R. D. Poulsen, A. D. Bond, M. A. S. Chevallier, B. B. Iversen, *J. Solid State Chem.* **2005**, *178*, 3342–3351.
[18] a) H. Ding, W. Chen, Q. Yue, J. S. Chen, S. N. Wang, *Chin. J. Chem.* **2003**, *21*, 1305–1308; b) J. Y. Sun, Y. M. Zhou, Q. R. Fang, Z. X. Chen, L. H. Weng, G. S. Zhu, S. L. Qiu, D. Y. Zhao, *Inorg. Chem.* **2006**, *45*, 8677–8684; c) M. Edgar, R. Mitchell, A. M. Z. Slawin, P. Lightfoot, P. A. Wright, *Chem. Eur. J.* **2001**, 5168–5175.
[19] H. Kumagai, M. A. Tanaka, K. Inoue, K. Takahashi, H. Kobayashi, S. Vilminot, M. Kurmoo, *Inorg. Chem.* **2007**, *46*, 5949–5956.
[20] S. S. Y. Chui, S. M. F. Lo, J. P. H. Charmant, A. G. Orpen, I. D. Williams, *Science* **1999**, *283*, 1148–1150.
[21] B. Panella, M. Hirscher, H. Pütter, U. Müller, *Adv. Funct. Mater.* **2006**, *16*, 520–524.
[22] O. Kahn, *Molecular Magnetism*, VCH, New York, NY, **1993**.
[23] S. C. Manna, J. Ribas, E. Zangrando, N. R. Chaudhuri, *Inorg. Chim. Acta* **2007**, *360*, 2589–2597.
[24] a) Durgaprasad, G. Sathyana, C. C. Patel, *Bull. Chem. Soc. Jpn.* **1971**, *44*, 316–322; b) T. C. Jao, I. Scott, D. Steele, *J. Mol. Spectrosc.* **1982**, *92*, 1–17.
[25] a) A. M. Heyns, *J. Mol. Struct.* **1985**, *127*, 9–20; b) L. Pranger, A. Goldstein, R. Tannenbaum, *Langmuir* **2005**, *21*, 5396–5404; c) G. Varsanyi, *Assignments for Vibrationals Spectra of Seven Hundred Benzene Derivatives, Vol. 1*, John Wiley & Sons, New York, **1974**, p. 107; d) G. N. R. Tripathi, S. J. Sheng, *J. Mol. Struct.* **1979**, *57*, 21–34.

Received: December 18, 2008
Published Online: April 21, 2009

